

Electronic transport in $\text{Ba}_{1-x}\text{K}_x\text{BiO}_3$ single crystals

J. H. Lee, K. Char, and Y. W. Park

Department of Physics and Condensed Matter Research Institute, Seoul National University, Seoul 151-742, Korea

L. Z. Zhao and D. B. Zhu

Department of Chemistry, Chinese Academy of Sciences, Beijing, China

G. C. McIntosh and A. B. Kaiser

Department of Physics, SCPS, Victoria University of Wellington, P.O. Box 600, Wellington, New Zealand

(Received 1 October 1999; revised manuscript received 11 January 2000)

We report measurements of the thermopower and resistivity of two superconducting $\text{Ba}_{1-x}\text{K}_x\text{BiO}_3$ single crystals with $x \sim 0.4$ (close to optimal doping), and analyze these data together with earlier data for K concentrations that span the accessible metallic and superconducting phase $0.37 < x < 0.55$. The thermopower S for temperatures below 120 K exhibits similar behavior to that seen for the cuprates close to optimal doping: the thermopower is positive for temperatures just above T_c but decreases with increasing temperature. A change of slope appears in the thermopower data at $T \sim 120\text{--}150$ K, with an increase in dS/dT above this temperature. We show that all the data can be accounted for by a two-band model similar to that used by Hashimoto *et al.* to explain the thermopower of the related superconductor, $\text{BaPb}_{0.75}\text{Bi}_{0.25}\text{O}_3$, and are consistent with the reported persistence of the charge-density-wave gap in the superconducting phase near the metal-semiconductor transition.

I. INTRODUCTION

The bismuthate superconductor, $\text{Ba}_{1-x}\text{K}_x\text{BiO}_3$ (BKBO),^{1,2} is often classed as a high-temperature superconductor, since its superconducting transition temperature ($T_c \sim 30$ K) is well above that of pre-1986 superconductors. BKBO is of considerable interest since it has several similarities to the cuprate superconductors apart from high T_c values: it is an oxide with a perovskite structure involving a low carrier density and in which superconductivity is observed near a metal-insulator transition.

Despite such similarities, there are also marked differences. In contrast to the planar structure of the cuprates, the superconducting phase of BKBO has a three-dimensional cubic structure.³ The undoped parent compound for BKBO (BaBiO_3) contains no magnetic ions but instead consists of an insulating charge-density-wave (CDW) phase.^{4,5} As potassium is substituted onto the Ba site, a metallic superconducting phase is formed for $0.37 < x < 0.55$. Another difference is that various evidence suggests that a more conventional BCS-type picture involving electron-phonon coupling is responsible for superconductivity in BKBO.⁶⁻¹¹ Given such similarities and differences, the study of BKBO is very worthwhile since a comparison with the cuprates may provide clues regarding mechanisms for high T_c . An understanding of the normal state formed above T_c is important for understanding the nature of the superconducting state. In particular, it is useful to study the normal state electronic transport properties of these materials in order to determine characteristics of the normal state carriers.

When BKBO crystals are optimally doped, their resistivity tends to vary approximately linearly with temperature, but with overdoping the resistivity above T_c takes on a higher power-law behavior.¹² A similar behavior is seen in

cuprate superconductors.¹³ (We note that single crystals or melt-processed¹⁴ BKBO are needed to observe the intrinsic metallic resistivity behavior, since the resistivity of ceramic BKBO samples¹⁵⁻¹⁷ appears to be dominated by grain boundaries and disorder.)

Regarding thermoelectric power, the high- T_c cuprates show remarkably systematic behavior.^{18,19} The in-plane thermopower, S , is positive just above T_c and then decreases approximately linearly with increasing temperature. As the hole carrier concentration is increased, the thermopower shifts to smaller values while still maintaining approximately the same slope as a function of temperature. In the overdoped limit, the cuprate thermopower is similar to that expected for the diffusion thermopower of a conventional metal in which the carriers are electrons, $S \propto -T$.

For BKBO, there appears to be only one set of previous thermopower data on single crystals.²⁰⁻²² These data, measured on crystals grown by Tang,²³ reveal a surprising similarity in the temperature range above T_c to the pattern of temperature dependence seen in the high- T_c cuprates. The main difference between the BKBO and cuprate thermopower data is that a knee appears in the BKBO data at a temperature $T \sim 150$ K with an upturn above this temperature. Previous measurements of BKBO thermopower on ceramic samples¹⁵⁻¹⁷ show somewhat varying behavior, but a change of slope as a function of temperature is also seen in these samples.

In this paper, we investigate further this intriguing behavior of the BKBO thermopower for the superconducting phase. We first report thermopower and resistivity measurements on two new BKBO crystals that provide independent confirmation of the behavior found for the one previous set of crystals measured.²⁰⁻²² We then analyze these data together with the earlier data set and show that a two-band

model accounts very well for all the available data on $\text{Ba}_{1-x}\text{K}_x\text{BiO}_3$ in the accessible metallic phase $0.37 < x < 0.55$ (superconductivity is also observed at low temperatures in this range).

II. EXPERIMENTAL DATA

Two $\text{Ba}_{0.6}\text{K}_{0.4}\text{BiO}_3$ single crystals were prepared using electrochemical synthesis. The starting materials, KOH, $\text{Ba}(\text{OH})_2 \cdot 8\text{H}_2\text{O}$ and Bi_2O_3 , were heated in a teflon crucible at 280°C . In order to grow single crystals electrochemically, platinum and gold wires were used for the anode and cathode, respectively. The applied current was typically ~ 4 mA and the crystal growth was performed at 280°C in air without stirring. A typical time for the electrochemical deposition was 22 h. One of the crystals (labeled as **c**) was prepared six months before the other (crystal **b**). The size of the crystals was approximately $3.6\text{ mm} \times 2.4\text{ mm} \times 2.0\text{ mm}$. For resistivity measurements, the standard four-probe method was used with silver wires attached to the samples using silver paste. For the thermopower measurements a standard differential thermocouple technique was used. The small size of the crystals and the very small magnitude of the measured thermopower means that measurement uncertainties are relatively large in relation to the thermopower magnitude.

We present our measurements for the new crystals **b** and **c** in Fig. 1 (resistivity) and in Fig. 2 (thermopower) together with earlier data from Subramaniam *et al.*²⁰ and Liu *et al.*²¹ The inset in Fig. 1 illustrates the decrease in T_c as the current increases. From the sharp low-current resistivity transition we estimate $T_c \approx 29$ K for crystal **b** and $T_c \approx 27$ K for crystal **c**, confirming that the crystals are near optimal doping.³

The resistivity and T_c value for our new crystal **b** are similar to those of crystal **a** for which the K concentration was measured to be $x \sim 0.38$ (corresponding to optimal doping),²⁰ but there is a tendency to a T^2 behavior in the resistivity just above T_c for our crystal **b**. The resistivity temperature dependence of our crystal **c** is similar to that of crystal **b** but the magnitude of the resistivity is lower; a rather variable magnitude of resistivity for BKBO crystals near optimal doping was also found in the earlier data set.²⁰ The earlier data for overdoped crystals **d** and **e** show depressed T_c values and a more pronounced nonlinear behavior in resistivity.²¹

As illustrated in Fig. 1, the resistivity of all the BKBO crystals has a temperature dependence of metallic character, with no clear evidence of any contribution to temperature dependence from semiconductorlike conduction as typically seen in ceramic samples.^{15–17} However, the magnitude of the resistivity is extremely high for a metallic system, indicating a small density of carriers as might be expected near a metal-insulator transition. The extrapolated residual resistivity is also a large fraction of the total resistivity at room temperature (approximately 0.3, or higher for crystal **a**), which suggests a large amount of disorder scattering is present. This presence of strong elastic scattering of carriers due to disorder may play a role in reducing the power of the temperature dependence due to scattering by phonons below the T^5 behavior seen in good metals with small elastic scattering, or the lower power behavior may arise from electron-electron scattering in a Fermi liquid.²⁴ We further discuss resistivity

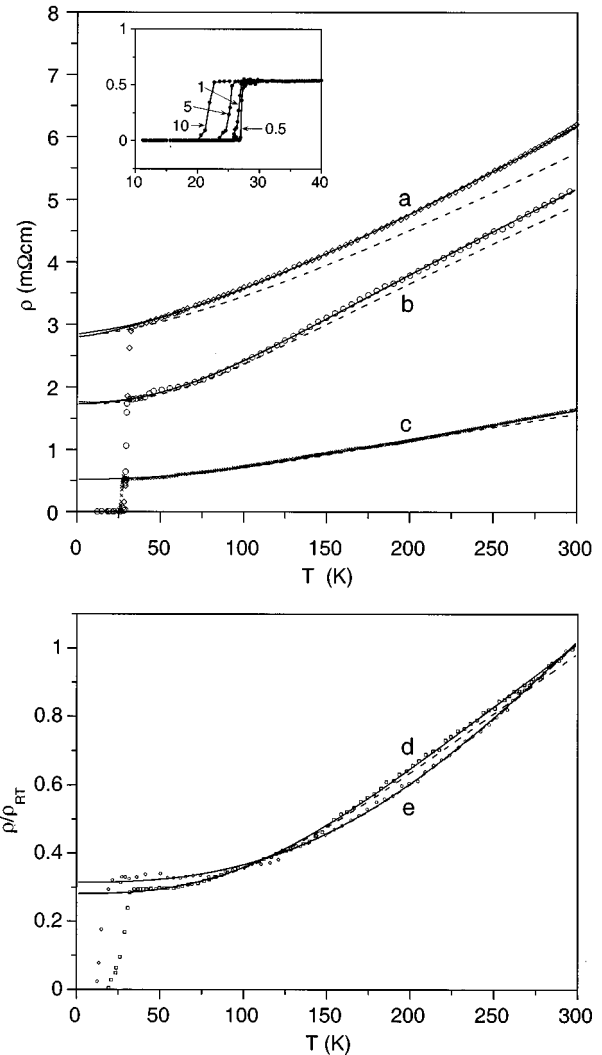


FIG. 1. Resistivity ρ of $\text{Ba}_{1-x}\text{K}_x\text{BiO}_3$ single crystals (normalized by the room temperature resistivity ρ_{RT} for crystals **d** and **e**). Samples **b** and **c** are our new crystals ($x \sim 0.4$), **a** is an optimally doped crystal ($x \sim 0.38$) measured by Subramaniam *et al.*, (Ref. 20), and **d** and **e** are overdoped crystals ($x \sim 0.5$ and $x \sim 0.55$, respectively) measured by Liu *et al.* (Ref. 21). The solid curves show fits of the generalized Bloch-Grüneisen function, Eq. (3). Dashed curves show the effects of including the hole band and the nonlinearity in energy-dependent conductivity for the same parameters as in the fit to Eq. (3); these shapes rescaled to fit the data are also shown by full curves but are essentially indistinguishable from the fit to Eq. (3). The inset shows the effect of current on T_c for crystal **c**; the labels indicate current in mA, with 1 mA corresponding to a current density of approximately 40 mA/cm^2 .

below after analyzing the thermopower data.

Our new thermopower data for crystals **b** and **c** in Fig. 2 confirm the key features of the earlier data set, namely a decrease in thermopower above T_c and an increase in dS/dT in the temperature range 120–150 K. The general consistency of the behavior for the different samples shown in Fig. 2 gives confidence that these basic features are in fact characteristic of BKBO thermopower behavior.

These data resemble the thermopower behavior seen for the high- T_c cuprates close to optimal doping. For temperatures just above T_c the thermopower is positive but then

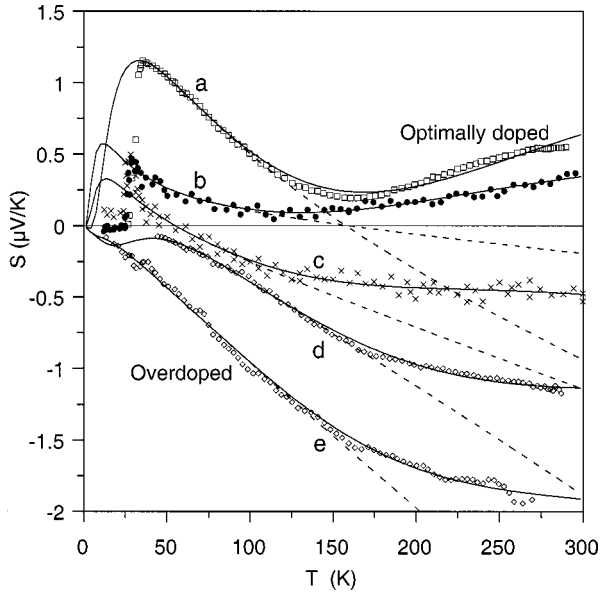


FIG. 2. Measured thermopower for our new $\text{Ba}_{1-x}\text{K}_x\text{BiO}_3$ crystals **b** and **c**, with data for the crystal **a** from Subramaniam *et al.* (Ref. 20) and for crystals **d** and **e** from Liu *et al.* (Ref. 21). The dashed curves are fits of Eqs. (1)–(7) (fitted only below 120 K), and the full curves are fits to Eqs. (1)–(6) and (8) for our proposed electron-hole two band model. Potassium concentrations x and fit parameters are listed in Table I.

decreases with increasing temperature. For $T \lesssim 120$ K, the slope $dS/dT \sim -0.005$ to $-0.01 \mu\text{V K}^{-2}$ has a much smaller magnitude than that seen for the cuprates.¹⁸ The thermopower magnitude is also smaller than in the cuprates or in the related superconductor $\text{BaPb}_{0.75}\text{Bi}_{0.25}\text{O}_3$,²⁵ and very small even compared to good metallic systems. Another difference from the high- T_c cuprates is that the increase in dS/dT above $T \sim 120$ – 150 K that we and previous workers observe in BKBO is typically not seen in the cuprates.

Given that the thermopower is increasing with decreasing temperature for optimally doped BKBO crystals, the normal-state thermopower must have a positive peak at low temperatures. This peak is suppressed below T_c by the presence of superconducting pairs but we surmise that it exists since the thermopower must tend to zero in the zero-temperature limit. As the hole carrier concentration is increased, the positive peak becomes reduced until, in the overdoped regime, the peak is completely lost. The remaining negative linear thermopower, $S \propto -T$, below 150 K is then typical of the diffusion thermopower expected in a conventional metallic system and very similar to the behavior of overdoped cuprates mentioned in the Introduction. The fact that the thermopower of our crystal **c** becomes negative at higher temperatures suggests that it is slightly overdoped compared to crystals **a** and **b**, in agreement with its slightly lower T_c value and smaller resistivity.

Unlike the cuprates, BKBO cannot be significantly underdoped to show a lower T_c while retaining itinerant carriers. Instead, at low temperatures BKBO shows a transition to a semiconducting orthorhombic phase as the K concentration x decreases below 0.37.³ The upper limit on x is set by the difficulty of synthesizing crystals with $x > 0.5$.^{3,12} Thus the

data in Fig. 2 that we analyze span the accessible metallic superconducting phase $0.37 < x < 0.55$ for BKBO.

III. TWO-BAND MODEL

We now consider an explanation for the thermopower behavior shown in Fig. 2. In view of the evidence for the conventional electron-phonon interaction as the origin of the superconductivity, we focus on conventional explanations. Given that the simple linear negative thermopower in the overdoped regime can be understood in terms of conventional metallic diffusion thermopower, there remain to be explained two main features of the thermopower data. One is the increasing positive thermopower peak as samples are progressively doped away from the overdoped regime, and the other is the knee occurring at $T \sim 120$ – 150 K.

It was pointed out earlier²⁰ that the relative similarity between thermopower in ceramic BKBO samples to that in crystals argues against phonon drag as the cause of the low-temperature thermopower peaks. This is because the increased disorder in the ceramics, demonstrated by their non-metallic resistivity behavior, would be expected to suppress phonon drag and therefore lead to a greater difference in thermopower behavior if phonon drag were a major factor in the crystals. The large residual scattering in all the crystal samples would also be expected to decrease phonon drag even in the crystals.

We therefore consider instead, an explanation in terms of electronlike and holelike contributions to the diffusion thermopower, following the general approach used by Hashimoto *et al.*²⁵ to account for thermopower in the closely related bismuthate superconductor $\text{BaPb}_{0.75}\text{Bi}_{0.25}\text{O}_3$. We infer from the extremely small thermopower of all $\text{Ba}_{1-x}\text{K}_x\text{BiO}_3$ samples in the concentration range for which superconductivity occurs that the Fermi surface is not strongly holelike or electronlike. This is particularly the case since, according to the Mott formula, free-electron-like metals with low carrier density are expected to have a large thermopower. The evolution of the thermopower near room temperature from positive with positive slope for some optimally doped samples, to negative with negative slope for overdoped samples, may reflect the evolution of part of the Fermi surface from slightly holelike to electronlike as K is substituted for Ba. Such a picture appears to be consistent with the band-structure calculations of Mattheiss and Hamann⁴ for ordered $\text{Ba}_{0.5}\text{K}_{0.5}\text{BiO}_3$, where the Fermi level appears near the middle of the upper $\text{Bi}(6s)\text{-O}(2p)$ band: substitution of monovalent K for divalent Ba could lower the Fermi level slightly and lead to more electronlike behavior.

In the parent compound, BaBiO_3 , a commensurate charge-density-wave distortion opens up a semiconductor gap, explaining its semiconducting properties,⁴ and this gap persists until $x \sim 0.37$ where the superconducting regime begins. Observations of x-ray superlattice reflections by Du *et al.*²⁶ indicate the presence of a charge-density wave, caused by the ordered disproportionation between nonequivalent Bi^{3+} and Bi^{5+} ions, even for the superconducting composition $x \sim 0.4$ in $\text{Ba}_{1-x}\text{K}_x\text{BiO}_3$. We, therefore, consider a contribution from a semiconductorlike hole band persisting in the superconducting regime (in addition to a me-

TABLE I. Parameter values obtained for the fits to the thermopower data shown in Fig. 2 using Eqs. (1)–(8). (Error estimates are obtained from the fitting procedure assuming random scatter of data points about the best-fit curves.) Approximate potassium concentrations x are also given for each crystal.

Data set	x	$\frac{\sigma_h(300 \text{ K})}{\sigma_e(300 \text{ K})}(\%)$	E_h (meV)	$c_e(\text{eV}^{-1})$	ε_c (meV)	β
a	0.38	8.05 ± 0.05	3.10 ± 0.05	0.252 ± 0.006	70.8 ± 0.7	0.086 ± 0.002
b	0.4	5.32 ± 0.04	1.03 ± 0.49	0.053 ± 0.015	64.2 ± 0.2	0.024 ± 0.002
c	0.4	3.67 ± 0.06	1.30 ± 0.97	0.184 ± 0.021	63.7 ± 0.2	0.029 ± 0.002
d	0.5	3.96 ± 0.04	7.79 ± 0.27	0.409 ± 0.019	102 ± 2	0.097 ± 0.007
e	0.55	0.70 ± 0.01	2.97 ± 0.80	0.417 ± 0.006	87.3 ± 2.5	0.085 ± 0.008

tallic term) as a possible explanation of the temperature dependence of thermopower.

To formulate a specific model, we start with the general expression for the overall thermopower for a two-band model, given by

$$S = \frac{\sigma_e}{\sigma} S_e + \frac{\sigma_h}{\sigma} S_h, \quad (1)$$

where S_e is the thermopower characteristic of the dominant metallic band and S_h is the thermopower of the holelike band. The contributions from S_e and S_h are each weighted by the respective conductivities, σ_e and σ_h . The overall conductivity, σ , is

$$\sigma = \sigma_e + \sigma_h. \quad (2)$$

We model the resistivity of a metallic band, $\rho_e = 1/\sigma_e$, using a generalized Bloch-Grüneisen formula which yields a T^p power-law behavior at low temperatures and gives a good representation of the measured resistivity of the crystal samples:

$$\rho_e = A + BT^p \int_0^{\theta/T} \frac{x^p}{(e^x - 1)(1 - e^{-x})} dx, \quad (3)$$

where A and B are constants and θ corresponds to an effective cutoff energy (the Debye temperature for scattering of carriers by phonons). Setting $p=2$ recovers the standard form of the Bloch-Grüneisen expression for electron-phonon scattering.²⁷ The values of the parameters used are those that give a fit to the resistivity data corresponding to the particular thermopower data we wish to study (the values of p vary from 1.3 for crystal **a** to 2.5 for crystal **e**).

For metallic thermopower we use the standard formula²⁸

$$S_e = \frac{1}{eT\sigma_e} \int (\varepsilon - \mu) \frac{\partial f_0}{\partial \varepsilon} \sigma_e(\varepsilon) d\varepsilon. \quad (4)$$

A linear metallic thermopower with a negative slope, appropriate for the overdoped regime, follows from the usual linear expansion for the energy-dependent conductivity, $\sigma_e(\varepsilon)$;

$$\sigma_e(\varepsilon) = 1 + c_e \varepsilon, \quad (5)$$

where energy ε is measured from the Fermi level, and $c_e > 0$ for electronlike behavior.

Following Hashimoto *et al.*,²⁵ we also consider a holelike band in which conduction is thermally activated, with conductivity given by

$$\sigma_h = \sigma_0 \exp(-E_h/T), \quad (6)$$

where E_h is the activation energy and σ_0 is a constant, and thermopower given by

$$S_h = |k/e|(E_h/T + C), \quad (7)$$

where C is a constant and $|k/e|$ has the standard value $|k/e| = 86.17 \mu\text{V K}^{-1}$. Such activated holes could possibly make a significant contribution to thermopower in a very low conductivity metal such as BKBO, with the contribution to thermopower being much larger than that to conductivity since the thermopower for semiconductor conduction is typically much larger than that for metallic conduction.

Using Eqs. (1)–(7) we can obtain reasonable fits to the BKBO thermopower data for temperatures $T \leq 120$ K, as shown by the dashed curves in Fig. 2. The positive thermopower peak at low temperatures arises from contributions from Eqs. (6) and (7) due to the hole carriers. On the one hand, the $1/T$ dependence in Eq. (7) causes the thermopower to increase with decreasing temperature but, as $T \rightarrow 0$, the weighting factor in Eq. (1) with conductivity given by Eq. (6) becomes extremely small and this causes the thermopower to decrease to zero as $T \rightarrow 0$.

From these fits we can determine, for each data set, the activation energy E_h , the relative contribution of localized carriers to transport at room temperature compared with metallic carriers, $\sigma_h(300 \text{ K})/\sigma_e(300 \text{ K})$, and the normalized slope of the linear energy dependence for the metallic wide band at the Fermi level, $c_e = d \ln \sigma_e(\varepsilon_F)/d\varepsilon$. Values for these parameters are given in Table I (the value of C was taken as zero, since it could not be adequately determined by fitting to the data). We see that the holes provide only a minor contribution to charge transport with $\sigma_h(300 \text{ K})/\sigma_e(300 \text{ K}) < 10\%$. Also, $\sigma_h(300 \text{ K})/\sigma_e(300 \text{ K})$ decreases as the samples become more overdoped. This is consistent with the positive thermopower peak decreasing and the semiconducting carriers becoming insignificant as the samples are doped away from the metal-insulator transition into the overdoped regime. Values obtained for the activation energy are $E_h < 10$ meV. This is very small as required for a contribution to conductivity at relatively low temperatures. We show below that this contribution to electronic transport, while af-

fecting thermopower, has little effect on the temperature dependence of the total conductivity.

As shown by the dashed curves in Fig. 2, the upturn seen in the data above 120 K is not given by the above model. For the $\text{BaPb}_{0.75}\text{Bi}_{0.25}\text{O}_3$ data of Hashimoto *et al.*,²⁵ there is no positive peak in the thermopower down to T_c , and the sharp increase in slope near 200 K is accounted for by a model similar to the above but with a greater activation energy for the hole conduction. In our case, only a modest change in slope is seen at around 120–150 K, which we can model by a simple extension of our model above. We find that this slope change is consistent with a nonlinearity in the energy-dependent conductivity $\sigma(\varepsilon)$, due to a nonlinear energy dependence of the density of states or other electronic parameters. There is a saddle point near the Fermi surface in the vicinity of the X point in the band-structure calculations of Mattheiss and Hamann⁴ that appears to be associated with a decrease in the density of states at higher energies. We model this by a change in the normalized energy-dependent conductivity for energies ε greater than a value ε_c :

$$\sigma(\varepsilon) = \begin{cases} 1 + c_M \varepsilon & \text{for } \varepsilon \leq \varepsilon_c \\ 1 - \beta + c_M \varepsilon & \text{for } \varepsilon > \varepsilon_c, \end{cases} \quad (8)$$

where β gives a constant decrease in $\sigma_e(\varepsilon)$ above ε_c .

With this nonlinearity incorporated into our model we obtain good fits to the BKBO thermopower data as shown by the solid curves in Fig. 2. Values obtained for ε_c and β for the various data sets are also given in Table I. These values were obtained with σ_0 , E_h and c_e held fixed at values obtained previously for fits to temperatures $T \leq 120$ K (dashed curves). We see that, in order to reproduce the knee, ε_c must occur at approximately 60–100 meV above the Fermi level. The larger values for the overdoped samples may reflect the movement of the Fermi level to lower electron energies as the K doping is increased. Interestingly, we find that a mobility loss of only 3–9% above ε_c is all that is needed to produce the knee at $T \sim 120$ –150 K for these data. The smallness of this effect means that the nonlinearity in $\sigma_e(\varepsilon)$ has little effect on the temperature dependence of resistivity.

The resistivity is also only slightly affected by the presence of semiconductor hole conduction. The dashed curves in Fig. 1, showing the effect on resistivity of including both the hole band term and the nonlinearity in energy-dependent conductivity, have essentially the same shape as the generalized Bloch-Grüneisen function, and when fitted to the data by adjusting the scaling parameters, A , B , and θ , give fits essentially identical to those of Eq. (3), shown by the full curves. Our thermopower model is therefore consistent with the resistivity data. In addition, the negative Hall coefficient¹² for the earlier BKBO crystals is also consistent with only a minor contribution to conductivity from the hole band. The lack of a systematic change in resistivity temperature dependence in the temperature range 120–150 K argues against explaining the thermopower upturn in terms of a structural transition, and in fact no transitions are reported in the range $0.37 < x < 0.55$.³

The detailed model we have used is not unique. For example, we find that placing a peak below the Fermi level

instead of the step in the energy-dependent conductivity could also account for the upturn in thermopower above 120–150 K (we have shown²⁹ that such a peak could account for the change in slope of the thermopower of a carbon nanotube mat sample). Another contribution to the upturn could come from electron-phonon renormalization effects involving high energy phonons.¹⁷ However, our calculations do show that a two-band model involving metallic electron and semiconductorlike hole conduction can account realistically for the observed behavior.

IV. CONCLUSION

We have made measurements of the thermopower and resistivity of two $\text{Ba}_{1-x}\text{K}_x\text{BiO}_3$ single crystals that confirm the general pattern reported in earlier data for the metallic and superconducting phase. For temperatures below ~ 120 K, the measured thermopower displays very similar behavior to that seen for high- T_c cuprates, but is smaller in magnitude. However, at $T \sim 120$ –150 K a knee appears in the BKBO thermopower data which is not seen for the cuprates.

We have shown that our thermopower and resistivity data sets and the earlier data for single crystals of BKBO can be accounted for by a conventional two-band model involving a metallic band with weakly electronic character, and a semiconductorlike hole band. The low-temperature thermopower peak in the samples near optimal doping for maximum T_c is associated with the contribution from the hole band which disappears as the system is doped away from the metal-insulator transition. Such behavior might be expected if a small energy gap or ‘‘pseudogap’’ associated with the CDW persists into the neighboring optimally doped superconducting regime for part of the Fermi surface, as suggested by x-ray diffraction experiments.²⁶ The disappearance of the positive thermopower peak for the overdoped region indicates that any remaining CDW gap disappears as the K concentration is increased to $x \sim 0.55$.

The upturn in the thermopower above 120–150 K is consistent with a small nonlinearity in the energy-dependent conductivity, possibly associated with band-structure effects. The measured resistivities and negative Hall coefficient are also consistent with this picture, since the hole band and energy-dependent conductivity nonlinearities have far less effect on the conductivity than on the thermopower.

ACKNOWLEDGMENTS

This work was supported by the international cooperative research program between the Korea Science and Engineering Foundation (KOSEF) and the Chinese Academy of Science (CAS), and also the Multi-National Cooperation Project on Quantum Transport in Synthetic Metals supported by the Korean Ministry of Science and Technology under Contract No. KISTEP 98-I-01-04-A-026. A.B.K. also acknowledges support from the Marsden Fund administered by the Royal Society of New Zealand. G.C.M. thanks D. C. Kim for helpful discussions.

- ¹L. F. Mattheiss, E. M. Gyorgy, and D. W. Johnson, Jr., Phys. Rev. B **37**, 3745 (1988).
- ²R. J. Cava, B. Batlogg, J. J. Krajewski, R. Farrow, L. W. Rupp, Jr., A. E. White, K. Short, W. F. Peck, and T. Kometani, Nature (London) **332**, 814 (1988).
- ³Shiyou Pei, J. D. Jorgensen, B. Dabrowski, D. G. Hinks, D. R. Richards, A. W. Mitchell, J. M. Newsam, S. K. Sinha, D. Vaknin, and A. J. Jacobson, Phys. Rev. B **41**, 4126 (1990).
- ⁴L. F. Mattheiss and D. R. Hamann, Phys. Rev. Lett. **60**, 2681 (1988).
- ⁵U. Hahn, G. Vielsack, and W. Weber, Phys. Rev. B **49**, 15 936 (1994).
- ⁶D. G. Hinks, B. Dabrowski, D. R. Richards, J. D. Jorgensen, S. Pei, and J. F. Zasadzinski, in *High Temperature Superconductors*, edited by J. R. Jorgensen *et al.*, Materials Research Symposia No. 156 (Materials Research Society, Pittsburgh, 1989), p. 357.
- ⁷M. A. Green, K. Prassides, P. Day, and D. A. Neumann, Synth. Met. **71**, 1619 (1995).
- ⁸S. J. Collocott, N. Savvides, and E. R. Vance, Phys. Rev. B **42**, 4794 (1990).
- ⁹H. Sato, T. Ido, S. Uchida, S. Tajima, M. Yoshida, K. Tanabe, K. Tatsuhara, and N. Miura, Phys. Rev. B **48**, 6617 (1993).
- ¹⁰Q. Huang, J. F. Zasadzinski, N. Tralshawala, K. E. Gray, D. G. Hinks, J. L. Peng, and R. L. Greene, Nature (London) **347**, 369 (1990).
- ¹¹M. Kosugi, J. Akimitsu, T. Uchida, M. Furuya, Y. Nagata, and T. Ekino, Physica C **229**, 389 (1994).
- ¹²S. F. Lee, J. Y. T. Wei, H. Y. Tang, T. R. Chien, M. K. Wu, and W. Y. Guan, Physica C **209**, 141 (1993).
- ¹³Y. Kubo, Y. Shimakawa, T. Manako, and H. Igarashi, Phys. Rev. B **43**, 7875 (1991).
- ¹⁴B. Dabrowski, S. Pei, Y. Zheng, D. G. Hinks, J. D. Jorgensen, D. R. Richards, and A. W. Mitchell, Ceram. Trans. **18**, 149 (1991).
- ¹⁵M. Sera, S. Kondoh, and M. Sato, Solid State Commun. **68**, 647 (1988).
- ¹⁶M. Pekala, R. Rataj, A. Pajaczkowska, and B. Gegenheimer, Phys. Status Solidi B **155**, K123 (1989).
- ¹⁷C. Uher, S. D. Peacor, and A. B. Kaiser, Phys. Rev. B **43**, 7955 (1991).
- ¹⁸A. B. Kaiser, Physica C **282-287**, 1251 (1997).
- ¹⁹A. B. Kaiser and G. C. McIntosh, Proc. SPIE **3481**, 75 (1998).
- ²⁰C. K. Subramaniam, A. B. Kaiser, and H. Y. Tang, Physica C **230**, 184 (1994).
- ²¹C.-J. Liu, H. Y. Tang, C. K. Subramaniam, and A. B. Kaiser, Physica C **282**, 1271 (1997).
- ²²A. B. Kaiser, C. K. Subramaniam, B. Ruck, and M. Paranthaman, Synth. Met. **71**, 1583 (1995).
- ²³H. Y. Tang, W. L. Chen, T. R. Chien, M. L. Norton, and M. K. Wu, Jpn. J. Appl. Phys., Part 2 **32**, L312 (1993).
- ²⁴J. S. Dugdale, *The Electrical Properties of Metals and Alloys* (Arnold, London, 1977).
- ²⁵T. Hashimoto, R. Hirasawa, T. Yoshida, Y. Yonemura, J. Mizusaki, and H. Tagawa, Phys. Rev. B **51**, 576 (1995).
- ²⁶C.-H. Du, P. D. Hatton, H. Y. Tang, and M. K. Wu, J. Phys.: Condens. Matter **6**, L575 (1994).
- ²⁷J. S. Blakemore, *Solid State Physics*, 2nd ed. (Cambridge University Press, Cambridge, 1985).
- ²⁸H. Fritzsche, Solid State Commun. **9**, 1813 (1971).
- ²⁹A. B. Kaiser, Y. W. Park, G. T. Kim, E. S. Choi, G. Düsberg, and S. Roth, Synth. Met. **103**, 2547 (1999).